



SYNTHESIS OF NA-A ZEOLITES FROM NATURAL AND THERMALLY ACTIVATED EGYPTIAN KAOLINITE: CHARACTERIZATION AND COMPETITIVE ADSORPTION OF COPPER IONS FROM AQUEOUS SOLUTIONS

Moaz K. Seliem*, E.A. Mohamed, A.Q. Selim, M. G. Shahien and Mostafa R. Abukhadra

Beni-Suef University, Faculty of Science, Geology Department, Egypt.

Received for publication: August 22, 2015; Accepted: September 17, 2015

Abstract: In this study, we prepared hydrated and dehydrated Na-zeolites under different conditions using sodium hydroxide (NaOH) and Egyptian kaolin. The synthetic zeolites were characterized by XRD, SEM, specific surface area and their adsorption behavior in the uptake of Cu^{2+} ions from aqueous solution were investigated, in order to compare the obtained results. The dehydrated Na-A zeolite showed well developed crystals and high surface area as compared to the hydrated Na-A zeolite. Batch adsorption studies showed that the maximum Cu^{2+} uptake percentage of dehydrated Na-A zeolite (94%) has been recorded after 5 min of contact time. On the other hand, the removal percentage of hydrated Na-A zeolite was 75% after 5 min reaching its maximum uptake percentage (97%) after 120 min. The mechanism of copper ions uptake by dehydrated Na-A zeolite followed ion exchange and precipitation while ion exchange was the main mechanism of adsorption in the case of hydrated Na-A zeolite. Copper adsorption kinetics by the synthetic Na-A zeolites was well fitted by pseudo-second-order kinetic model with R^2 greater than 0.99. Equilibrium sorption isotherms of Cu^{2+} ions by the synthetic zeolites were explained using the Langmuir and Freundlich isotherms models.

Key words: Natural zeolite; Synthetic zeolite A; Heavy metals; Water treatment

INTRODUCTION

Rapid urbanization, industrialization and economic development in recent years lead to a continuous influx of toxic materials such as heavy metals into a water body which frequently causes water pollution. Small amounts of naturally occurring heavy metals such as zinc (Zn), copper (Cu), lead (Pb) and cobalt (Co) are common in our environment and they are necessary to our health (Qiu and Zheng, 2009). But high concentrations of these heavy metals are dangerous for living organisms due to their toxicity, stability and tendency to accumulate in the environment (Kragovic, *et al.*, 2013). The accumulation of heavy metals over time in human bodies can cause severe damage of kidney, liver, reproductive system, lungs, blood composition and sometimes leads to cancer (Jamil, *et al.*, 2010). However copper ion is considered as an essential nutrient, its level above 1.3 mg/L with time leads to kidney and liver damage of human (Ennigrou, *et al.*, 2014). Chemical precipitation, ion exchange, neutralization, reduction and adsorption are used as different processes to uptake heavy metals from contaminated water (Kurniawan, *et al.*, 2006). Removal of heavy metals by adsorption process is preferred because it is very effective, economic, versatile and simple (Zhu, *et al.*, 2013). Among the adsorbents materials, zeolites were recommended because of their unique porous structure, high surface areas and low costs (Breck, 1974; Ibrahim, *et al.*, 2010).

Zeolite molecular sieves are crystalline microporous aluminosilicates with an indefinitely extending three-dimensional network of AlO_4 and SiO_4 tetrahedrons linked by sharing of oxygen atoms (Chaisena and Rangsrivatananon, 2005). The aluminum ion is small enough to occupy the position in the center of the tetrahedron of four oxygen atoms. Isomorphous replacement of Si^{4+} by Al^{3+} can take place and consequently, a net negative charge results. Therefore, cations such as Ca^{2+} , Na^+ or K^+ are usually found to balance the excess negative charge. These cations are

exchangeable with certain cations in solutions such as copper, lead, zinc and cadmium (Ibrahim, *et al.*, 2010). Zeolites may be formed through natural geological processes or can be synthesized in the laboratory. Man-made zeolites are usually synthesized under hydrothermal conditions from basic aluminosilicate precursor gels at elevated high temperatures (Youssef, *et al.*, 2008; Mousavi, *et al.*, 2013). Zeolites were synthesized using different materials such as carbonized rice husk (Katsuki, *et al.*, 2005), low-grade natural kaolin (Ma, *et al.*, 2014), natural and modified diatomite (Chaisena and Rangsrivatananon, 2005), kaolinite (Belviso, *et al.*, 2013), rice husk (Cheng *et al.*, 2012), rice husk ash and metakaolin (Atta, *et al.*, 2012), fly ash (Qiu and Zheng, 2009), paper sludge ash (Wajima, *et al.*, 2006), chrysotile and rice husk (Petkowicz, *et al.*, 2008) and rectorite mineral (Liu *et al.*, 2014). The A-type zeolite, one of the most common synthetic zeolites, has various applications in industry as catalysis, separation, ion exchange and adsorption (Xing-dong, *et al.*, 2013).

Kaolinite with a chemical formula $\text{Al}_2\text{Si}_2\text{O}_5(\text{OH})_4$ has a typical two-layered structure, where the T:O ratio = 1:1. Thermal activation in the range of 600-900°C leads to liberation of hydroxyl water from kaolinite forming metakaolinite as amorphous dehydroxylated aluminosilicate form. Since the Si/Al ratio is near to the unity in kaolinite and metakaolinite which is close agreement with that of zeolite A, these materials are frequently used as starting material for the synthesis of zeolite A (Youssef, *et al.*, 2008).

The natural deposits of zeolites are nearly absent in Egypt. This is why we have to go to the synthetic forms using cheap and available raw materials. To the best of our knowledge, the adsorption characteristics and the mechanism of dehydrated Na-A zeolite for the uptake of copper ions as compared to hydrated Na-A zeolite have not been studied so far. However the uptake of heavy metals by natural zeolite has been previously studied by many authors,

*Corresponding Author:

Moaz K. Seliem,
Lecturer,
Beni-Suef University,
Faculty of Science,
Geology Department, Egypt.

natural phillipsite was taken in this study just to light up the difference between the natural and synthetic zeolites. Thus, the main objectives of this work were: (a) to prepare and characterize dehydrated and hydrated Na-A zeolites from Egyptian kaolin clay sample, (b) to compare the uptake potential of copper ion from aqueous solution by the synthetic and natural zeolites, and (c) to study the adsorption behavior and the mechanisms of copper ion uptake by fitting the experimental data to different kinetics and isotherms models.

MATERIALS AND METHODS

Materials

The starting kaolinite clay sample used in the present study has a chemical composition of 46% SiO₂, 34% Al₂O₃, 3.2% TiO₂, 1.8% Fe₂O₃, 0.1% MgO, 0.6% CaO, 0.3% Na₂O, 0.05% K₂O and ignition loss nearly 14%. The alkali hydroxide used in the synthesis of zeolite A is NaOH (Alfa Aesar, purity: 97%). In addition, a natural zeolite (phillipsite-K) with a composition of (K,Na)₂(Si,Al)₈O₁₆·4H₂O was obtained from Mukeihlat area, Syria. This K-rich phillipsite zeolite was referred as (ZN). Copper acetate monohydrated supplied by Aldrich chemical Co. (purity > 98%) was used as a source of copper ion.

Synthesis of hydrated Na-A zeolite

A certain amount (nearly 10 g) of the raw Egyptian kaolin was subjected to calcination at high temperature of about 650°C for 5 h to obtain metakaolinite as amorphous and more reactive product. Hydrated Na-A zeolite was synthesized by adding 3g of metakaolinite to a solution contains 6g of sodium hydroxide and 50 ml distilled water. The mixture was subjected to a continuous vigorous stirring overnight at room temperature. After stirring, the mixture was transferred to 125ml stainless steel Parr reactors and heated in an oven at 90°C for 4 h. After hydrothermal treatment, the vessels were cooled down to room temperature. The contents from Teflon vessels were centrifuged to separate solids and solutions. Then, the solid products were washed with distilled water to remove the excess alkalinity and dried at 65°C. Hydrated Na-A zeolite synthesized by using this method was labeled (ZH).

Synthesis of dehydrated Na-A zeolite

To prepare dehydrated Na-A zeolite, 6g of the raw kaolinite was heated with 7.2g of NaOH 650°C for 5 h. The resultant fused mixture was cooled and ground with a mortar and pestle for a few minutes. The powder was mixed with 100 ml distilled water and stirred at temperature 70 °C for 2 h, then the solution was transferred to autoclave and treated at temperature 90°C for 4 h. After treatment, the solid part was separated by centrifugation, washed with distilled water and dried at 60°C overnight. Dehydrated Na-A zeolite prepared by this method was labeled (ZF).

Sample characterization

X-ray powder diffraction patterns were obtained using a Philips APD-3720 diffractometer with Cu K α radiation, operated at 20 mA and 40 kV in the 2 θ range of 5–70 at a scanning speed of 5°/min. The morphology of the studied natural and synthetic zeolites was studied by

scanning electron microscopy (SEM) technique (JSM-6510, JEOL, Tokyo, Japan). Particle size analyses and surface areas of the Na-A zeolites were determined by BT-2001 (wet) laser particle size analyzer device.

Batch adsorption and kinetic studies

Experiments to determine adsorption kinetics of copper (II) by the as-synthetic and natural zeolites were conducted by batch method at room temperature as follows: A fixed amount (0.4 g) of each dry adsorbent was mixed with 200 ml of 1mM of copper acetate monohydrated in a volumetric flask for 5 min, 30 min, 2 h, 8 h and 24 h with continuous agitating using orbital shaker. Before adding the zeolite samples, the solutions were acidified to avoid cation precipitation. The initial pH values of the studied solutions were adjusted to 6 \pm 0.2 (Qiu and Zheng, 2009). After equilibration, the solid and the solution phases were separated by centrifugation. Then, 150 ml of each liquid was collected in clean plastic bottle for determining the concentration of copper using inductively coupled plasma mass spectrometry (ICP-MS). The pH value of each collected liquid was examined and re-adjusted at each time interval by adding drops of nitric acid. The amount of copper adsorption onto the zeolites q_t (mg/g) at any time and removal efficiency (metal ion, removal %) were calculated as follows:

$$q_t = \frac{V(C_0 - C_t)}{m} \quad (1)$$

$$\text{Metal ion removal, \%} = 100 (C_0 - C_t) / C_0 \quad (2)$$

Where, C_0 and C_t are the ion concentrations in the initial solution and the solution after equilibration of heavy metal ions, respectively. V is the volume of solution in (L) and m is the mass of sorbent (gm).

Isotherm studies

The isotherms of copper ion adsorption by the studied as-synthetic and natural zeolites were determined using an initial concentration range from 0.5 to 2.5mM of Copper acetate monohydrated. A fixed amount (0.4 g) of ZN, ZH and ZF was mixed with 150 ml of 0.5, 1, 1.5, 2 or 2.5mM of copper acetate monohydrated by an orbital shaker for 24 h. After equilibration, the suspensions were centrifuged, solids and solutions were separated and the solutions were collected in clean plastic bottles. The concentrations of copper ion were determined in all solutions by using inductively coupled plasma mass spectrometry (ICP-MS).

RESULTS AND DISCUSSION

X-ray diffraction (XRD) results

The X-ray diffraction patterns of the used natural Egyptian kaolin and treated metakaolin are shown in Fig.1. Untreated kaolin clay sample was characterized by the presence of the main peaks of kaolinite and quartz while metakaolin was characterized by the absence of the main diffraction peaks of kaolin at 2 θ values of 12.34° and 24.64° (Gougazeh and Buhl, 2014). The main crystalline phase in metakaolin corresponds to the presence of quartz (Fig.1). The X-ray patterns of the natural and synthetic zeolite samples are shown in (Fig.2). Phillipsite-K and calcite represent the main crystalline phases in natural zeolite (ZN).

From Fig. 2, the crystalline phases of the synthesized products (ZH and ZF) correspond to the main peaks of zeolite A at 2θ values of 7.2° , 10.3° , 12.6° , 16.2° , 21.8° , 24° , 26.2° , 27.2° , 30° , 30.9° , 31.1° , 32.6° , 33.4° and 34.3° that were reported by (Treacy and Higgins, 2001). The sharp diffraction peaks in ZF indicate a high degree of crystallinity, as compared to ZH (Fig.2).

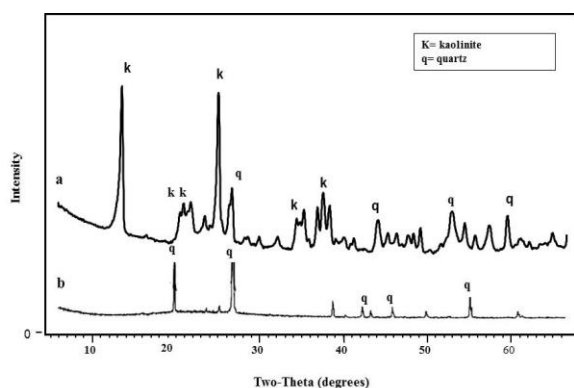


Figure 1: XRD patterns of (A) Egyptian kaolin and (B) Metakaolin at 650°C . Note the presence of the two main kaolinite clay mineral at 2θ values of 12.34° and 24.64° in the Egyptian kaolin (A) while absence of the main diffraction peaks of kaolin after treatment at 650°C in the metakaolin (B). Quartz was detected in untreated and treated kaolin samples.

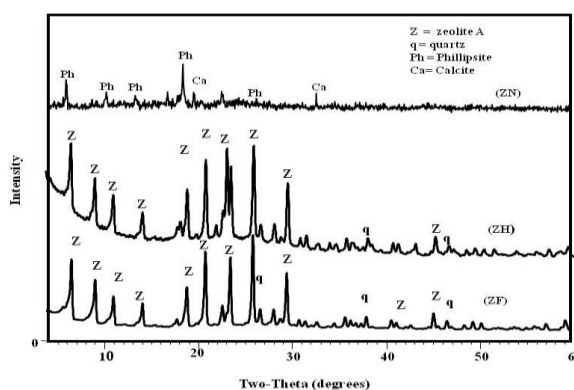


Figure 2: XRD patterns of natural zeolite (ZN) and synthetic zeolites A (ZH) and (ZF). Note Phillipsite-K and calcite are the main crystalline phases in natural zeolite (ZN) while the main peaks recorded at 2θ values of 7.2° , 10.3° , 12.6° , 16.2° , 21.8° , 24° , 26.2° , 27.2° , 30° , 30.9° , 31.1° , 32.6° , 33.4° and 34.3° refer to the synthetic zeolites (ZH and ZF).

Scanning electron microscopy (SEM) results

Fig. 3 shows the SEM images of both natural and synthetic zeolite samples. The natural zeolite was characterized by the presence of prismatic crystals of phillipsite-K (Fig. 3a). SEM images of ZH and ZF show the cubic crystals of the synthetic Na-A zeolite (Fig. 3b and c); however, the crystals are well developed in the ZF (Fig. 3c). The appearance of more cubic crystals with well-developed crystalline faces in ZF supports the presence of more sharp reflection peaks detected by X-ray diffraction (Fig. 2). The SEM results of the present work are similar to those

previously reported by (Belviso, *et al.*, 2013; Youssef, *et al.*, 2008; Mohamed, *et al.*, 2009; Gougazeh and Buhl, 2014).

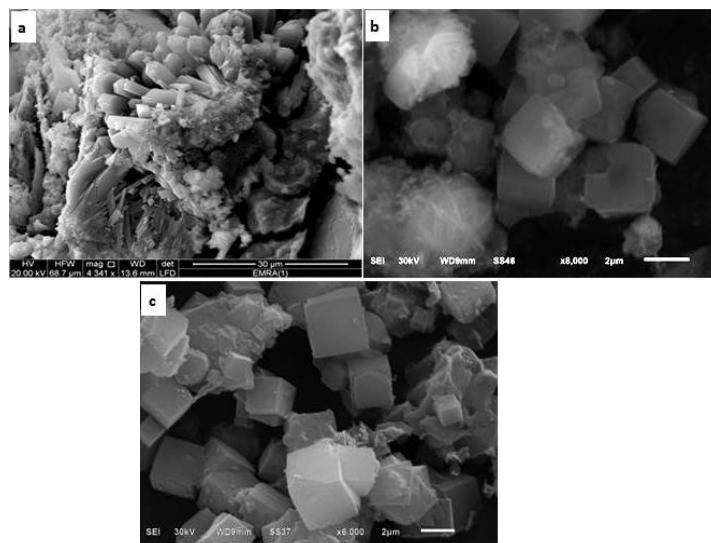


Fig. 3: Scanning electron micrographs of natural and synthetic zeolites A. ZN (a), ZH (b) and ZF (c). ZN is characterized by the presence of prismatic crystals of phillipsite-K (3a). (ZH) shows particles with irregular morphology associated with well-developed crystals (3b). (ZF) shows well developed cubic crystals with sharp edges and smooth surfaces (3c)

Particle size distribution and surface area

The particle size analyses of the studied synthetic zeolites showed that the ZF has particle size distribution as 98% less than $27\mu\text{m}$, 80% less than $15\mu\text{m}$, and 50% less than $5\mu\text{m}$, where the ZH has particle size distribution as 98% less than $49\mu\text{m}$, 80% less than $20\mu\text{m}$, and 50% less than $9\mu\text{m}$. The surface area measurements of the synthetic zeolites gave values of $189\text{ m}^2/\text{g}$ and $125\text{ m}^2/\text{g}$ for ZF and ZH, respectively.

Effect of contact time and adsorption kinetics

The removal efficiency of natural and synthetic zeolites for copper ion after contact time ranging from 5 min to 24 h was given in (Table, 1 and Fig. 4). The uptake percentage of copper ion by natural zeolite (ZN) increased from 46% to 92.5% by increasing the shaking time from 5 min to 120 min. This is may be related to the presence of calcite mineral in natural zeolite (Pitcher *et al.*, 2004). The contribution of calcite mineral in the uptake of cooper ion is related to the pH of solution which gave values of 6.2 and 8.3 after contact times of 5 min and 120 min, respectively (Table 1). Therefore, more surface active sites will be available for more copper ion uptake after 2 h of shaking time. After 120 min, the removal efficiency of copper was nearly constant, attained equilibrium within 120 min (Table 1).

Table 1: The removal efficiency and the amount of copper sorbed onto the studied natural and synthetic zeolites at different contact times.

Zeolite type	Time (min)	Metal ion removal (%)	q_t (mg/g)	pH
ZN	5	46	14.6	6.2
ZN	30	86	27.14	7.47
ZN	120	92.5	29.10	8.3
ZN	480	93	29.3	7.54
ZN	1440	93.5	29.34	7.20
ZH	5	75	23.54	10.22
ZH	30	96	30.13	10.29
ZH	120	97	30.5	10.71
ZH	480	93.5	29.46	10.31
ZH	1440	91	28.67	9.92
ZF	5	94	29.61	9.7
ZF	30	89	28.15	9.45
ZF	120	89	27.96	9.3
ZF	480	87	27.36	9.22
ZF	1440	87	27.40	9.15

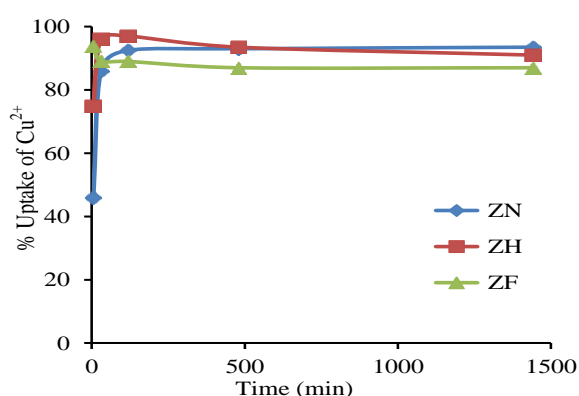


Fig. 4: Kinetic curves of copper ion uptake by the studied zeolites. The removal efficiency of natural (ZN) and synthetic zeolites (ZH, ZF) for copper ion after shaking time ranging from 5 min to 24 h.

The removal of copper by natural zeolite showed two distinct stages of adsorption with time (Fig. 4). The first stage (1 min <math>t < 120\text{ min}</math>) was characterized by a steep slope due to the rapid uptake rate during this stage (Seliem, *et al.*, 2013). The second stage (after 120 min) was signified by a gentle slope as a result of decreasing in the adsorption rate, i.e. equilibrium was attained (El-Mekkawi and Selim, 2014). Equilibrium was achieved due to the decreasing in the available active adsorption sites on the adsorbent and therefore, transfer of the adsorbate molecules from solution to the external surface of adsorbent became limited (Mehdizadeh, *et al.*, 2014). Concerning the synthetic ZH, the removal efficiency for Cu^{2+} increased from 75% to 96% with increasing time from 5 min to 30 min, (Table 1). As can be seen in Fig. 4, an appreciable stabilization trend attaining by increasing time from 30 min to 120 min, followed by slight decreasing to the end of shaking time. Decreasing the copper uptake by adsorbent may be related to the decrease in the number of active adsorption sites as well as copper concentration (Mishra and Patel, 2009). On the other hand, ZF gave the maximum value of uptake percentage (94%) after 5 min, followed by slight decreasing with increasing time to 24 h (Fig. 4). The abrupt decreasing in copper concentration during the first 5 min of contact time can be explained as a consequence of a very fast diffusion of the copper species from the aqueous solution

to the active sites of the dehydrated Na-A zeolite (Vacamier, *et al.*, 2001). In addition, no appreciable increase was observed after 5 min which proves the saturation of the active sites in ZF. The % uptake of copper was high (94%) in ZF as compared to ZH (75%) after shaking time 5 min. This may be attributed to the tendency of some of ZH particles to accumulate forming agglomerated particles (Fig. 5). Such aggregation would lead to decreasing in the particle size distribution and total surface area of ZH compared to ZF. In order to study the mechanism that control the adsorption process, the Lagergren pseudo-second order kinetic model was applied in this study. This model was found to be more common in prediction of the behaviour over the whole range of sorption (Kragovic, *et al.*, 2013). The pseudo-second order process can be written as follows:

$$\frac{t}{q_e} = \frac{1}{k_2 q_e^2} + \frac{t}{q_e} \quad (3)$$

Where, q_e is the equilibrium adsorption uptake of heavy metal ion (mg/g), q_t is the amount of copper adsorbed at time t (mg/g) and k_2 is the rate constant of second-order adsorption ($\text{g mg}^{-1} \text{min}^{-1}$). Thus, by plotting t/q_t versus t , k_2 and q_e values can be determined (Table 2). A good agreement of the experimental data with the second-order kinetic model was obtained (Fig. 6).

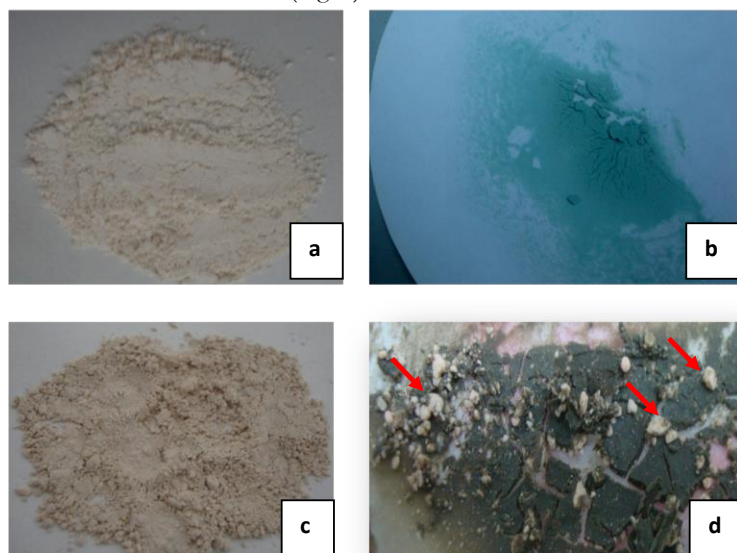


Fig.5: Photograph shows the colours of the studied Na-A zeolites before and after treatment at contact time 5 min: (ZF) a, b and (ZH) c, d (the red arrows refer to the presence of agglomeration of ZH particles). Note; the difference of the powder colour after treatment, the dehydrated Na-A zeolite has the green colour of the copper solution (b).

Table 2: Kinetic parameters for adsorption rate expressions.

Adsorbent	Second-order kinetic mode		
	k_2 (g/mg min)	q_e (Cal) (mg/g)	R^2
ZN	0.12×10^{-3}	29.41	0.9999
ZH	0.70×10^{-3}	28.08	0.9998
ZF	2.2×10^{-3}	27.44	0.9999

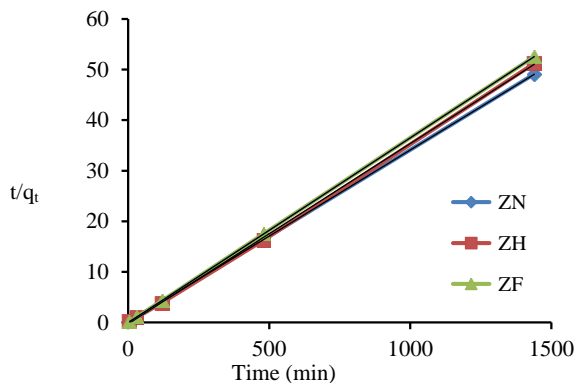


Fig.6: Plots for second-order model for copper ion uptake by ZN, ZH and ZF. Note the concordance of the experimental data with the second-order kinetic model obtained for both natural and synthetic zeolite.

The correlation coefficients are greater than 0.99 for both natural and synthetic zeolite, which suggest a strong relationship between the parameters and also explains that the process follows pseudo-second-order model. The higher k_2 values for synthetic zeolites indicates a faster increase in the amount of sorbed Cu^{2+} as compared to natural zeolite (Zeng, *et al.*, 2010). The adsorption process involves transportation of the solute molecules from the aqueous solution to the surfaces of the solid particles followed by intra-particle diffusion/transport process (Demiral and Gunduzoglu, 2010). The intra-particle diffusion can be written as follows:

$$q_t = k_p t^{1/2} + C \tag{4}$$

Where, k_p is the rate constant of intra-particle diffusion ($\text{mg g}^{-1} \text{min}^{-1/2}$) and was determined from the slopes of the lines in (Fig.7) and C is the intercept related to the thickness of the boundary layer. According to this model, if the plot of uptake, q_t , versus the square root of time, $t^{1/2}$ is linear and passes through the origin, then intra-particle diffusion is the only rate controlling step. As shown in Fig.7, the plot does not pass through the origin and exhibited multi-linear plots. Therefore, the intra-particle diffusion is not the only rate limiting step in the whole adsorption process (Seliem, *et al.*, 2013).

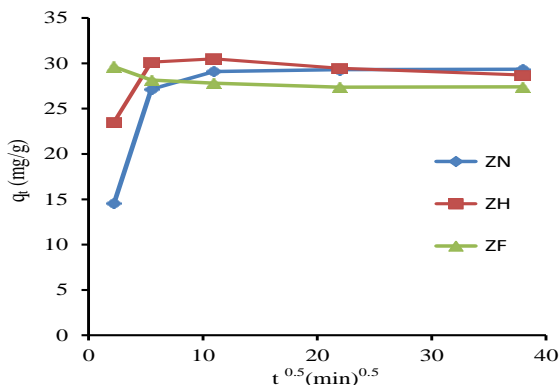


Fig. 7: Intraparticle diffusion model of copper adsorption by ZN, ZH and ZF. The plot of uptake, q_t , versus the square root of time, $t^{1/2}$ does not pass through the origin and exhibited multi-linear plots.

pH control of copper ion uptake

The pH of the solution is considered as an important controlling parameter in the adsorption process. At low value of pH, the surface of adsorbent was surrounded by protons that compete with metal ions and therefore, the adsorption of metal ion onto the surface of adsorbent decreases (Zhu, *et al.*, 2013). By increasing the solution pH, the surface of adsorbent was characterized by the presence of negative charges and therefore, the adsorption increases when the metal species have positive charges or neutral (Rao, *et al.*, 2008). The pH of the solutions after each contact time was recorded as shown in (see table 1). It was found that the pH value increased during the adsorption process by increasing contact time from 5 min to 120 min and gradually decreased to the end of shaking time for both of ZN and ZH (Fig.8). The pH values of solutions are matching with the % uptake of copper ion at each contact time (Table 1). On the other hand, the maximum pH value in ZF was recorded after 5 min and continuously decreased by increasing contact time to 24 h. By increasing pH, more negatively charged surface sites will be available which facilitates more adsorption of copper ion (Zhang, *et al.*, 2011). Therefore, copper may form copper hydroxyl species with OH^- groups such as $\text{Cu}(\text{OH})_2$, $\text{Cu}(\text{OH})_3^{2-}$ and $\text{Cu}(\text{OH})_4^{2-}$ which may participate in the adsorption process and participate onto the structures of zeolites preventing further adsorption (Oren and Kaya, 2006). The best values of the uptake of copper ion were recorded at pH values of 10.7 and 9.7 for ZH and ZF, respectively (Table 1). This has been supported by the difference in Na concentration in the solutions with values of 106.4 mg/L and 41.9 mg/L for the ZH and ZF, respectively. This indicates that the mechanism of copper ions uptake in ZH is mainly related to cation exchange, while the copper ions adsorption onto ZF may be related to a combination of ion exchange and precipitation mechanisms. This may reflect the changing of dehydrated Na-A zeolite to green color after 5 min of shaking time (Fig.5b).

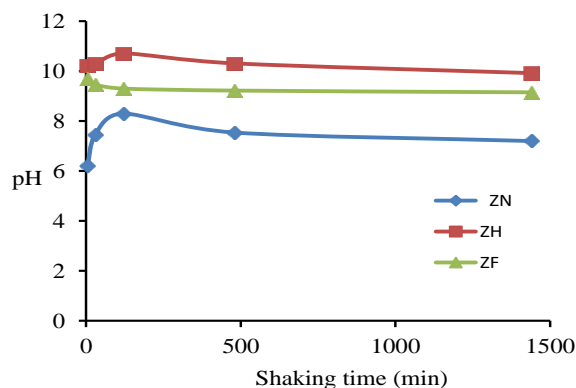


Fig. 8: pH of the solution after shaking time ranging from 5 min to 24 h. The pH values of the solutions were determined after contact time ranging from 5 min to one day of equilibrium.

Adsorption isotherms studies

Adsorption isotherms indicate the distribution of adsorbate between solution and adsorbent at the equilibrium state of the adsorption process. The type of

adsorption isotherm model is very important in order to understand the adsorption behavior for solid-liquid adsorption system (Wang, *et al.*, 2007). In the present study, Langmuir and Freundlich models were tested to study the adsorption behavior of copper ion as these two are the most commonly used. Based on the Langmuir theory, there are specific adsorption sites on the surface which become saturated after monolayer adsorption of sorbate is achieved and there is no significant interaction among adsorbed species (Hoda, *et al.*, 2006; El-Mekkawi and Selim, 2014; Seliem, *et al.*, 2013; Bagherifam, *et al.*, 2014). The Langmuir model is expressed as follows:

$$\frac{C_e}{q_e} = \frac{1}{bq_{max}} + \frac{C_e}{q_{max}} \quad (5)$$

Where, C_e is the equilibrium concentration of the remaining solute in the solution (mg/L), q_e is the amount of the solute adsorbed per mass unit of adsorbent at equilibrium (mg/g), q_{max} is the amount of adsorbate per mass unit of adsorbent at complete monolayer coverage (mmol/g), and b (L/mg) is a Langmuir constant. The q_{max} and b values were calculated from the slopes ($1/q_{max}$) and intercepts ($1/bq_{max}$) of linear plots of C_e/q_e versus C_e (Fig.9). The Langmuir isotherm parameters are given in Table 3. Linear plots of C_e/q_e versus C_e were found to be linear with good correlation coefficients greater than 0.97 that indicate the applicability of Langmuir model in the present study. One of the essential characteristics of Langmuir isotherm could be expressed by a dimensionless constant called equilibrium parameter R_L which is determined as follows:

$$R_L = 1/(1 + bC_0) \quad (6)$$

Where, b is a Langmuir constant and C_0 is the initial concentration. The value of R_L was calculated using the above expression. The values of R_L indicate the nature of the adsorption process (Lian *et al.*, 2009).

- $R_L > 1$ for unfavorable adsorption,
- $R_L = 1$ for linear adsorption,
- $0 < R_L < 1$ for favorable adsorption, and
- $R_L = 0$ for irreversible adsorption.

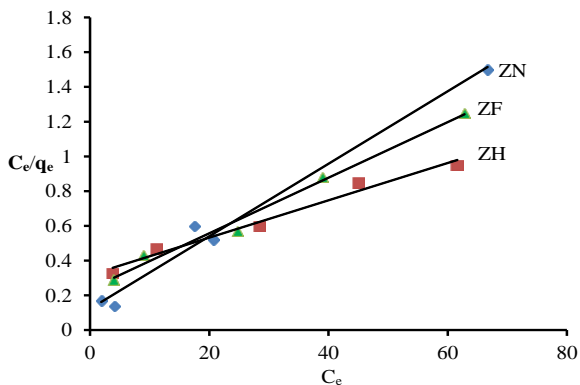


Fig. 9: Langmuir plots for the copper ion uptake by ZN, ZH and ZF. Linear plots of C_e/q_e versus C_e were found to be linear with good correlation coefficients ranging from 0.97 to 0.98., indicate the applicability of Langmuir model in the present study.

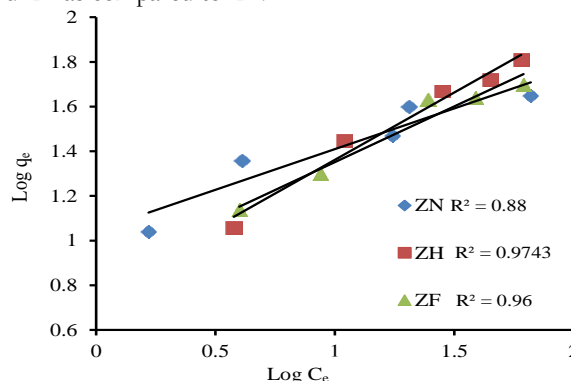
Table 3: Langmuir parameters for cooper ion uptake by the studied zeolites

Sample	Isotherm Parameters		
	q_{max} (m mol/g)	b (L/mg)	R^2
ZN	0.718	0.169	0.984
ZH	1.41	0.034	0.987
ZF	0.94	0.067	0.978

The R_L -values for the adsorption of natural zeolite are in the range of (0.034–0.149) while R_L -values for the adsorption of synthetic zeolites are in the range of (0.001–0.009). Based on the R_L -values of the studied samples, $R_L < 1$, indicating favorable adsorption process. The Freundlich isotherm model can be used to describe the non-ideal adsorption of a heterogeneous system and reversible adsorption (Wang and Zhu, 2006). This model states that reactions take place in several sorption sites and as the amount of solute adsorbed rises, the binding surface energy decreases exponentially which means multilayer sorption (Bagherifam, *et al.*, 2014). The Freundlich isotherm is expressed as follows:

$$\log q_e = \log K_F + 1/n \log C_e \quad (7)$$

Fig.10: Freundlich isotherm for copper ion uptake by ZN, ZH and ZF. A plot of $\log(q_e)$ vs. $\log(C_e)$ for the studied zeolite samples shows good correlation coefficients in ZH and ZF as compared to ZN.



Where, K_F and n are the Freundlich constants related to adsorption capacity and intensity, respectively. The values of K_F and $1/n$ are determined from the intercept and slope of the linear regressions. A value for n above one indicates a normal Freundlich isotherm while n below one refers to a cooperative adsorption (Amin, 2008; Vimonses, *et al.*, 2009). A plot of $\log(q_e)$ vs. $\log(C_e)$ for the studied zeolite samples is shown in (Fig. 10). The n values for the studied samples are in the range from 1.66 to 2.72 (i.e., more than 1), therefore, the adsorption of copper fits a normal Freundlich adsorption model.

CONCLUSIONS

The uptake of copper ion from aqueous solution at contact time ranging from 5 min to 24 h was studied by natural K-phillipsite zeolite and the studied Na-A synthetic zeolites. The highest amount of the uptake of copper ion after 120 min was given by the natural zeolite. But the best exposure times for the removal of copper ion were found to be 30 min and 5 min for Na-A hydrated zeolite and Na-A dehydrated zeolite, respectively. The mechanisms of cooper

ions uptake were mainly attributed to ion exchange and precipitation in the Na-A dehydrated zeolites and ion exchange in the Na-A hydrated zeolite. The adsorption characteristics and the mechanisms of copper removal followed pseudo-second-order kinetics and the applied isotherms models. Further detailed studies are needed, however, to understand the effect of many factors such as zeolite dose, competitive ions, is recommended.

ACKNOWLEDGEMENTS

The authors thank the support unit and project finance, Beni-Suef University, Egypt for financially supporting this study. The authors are also grateful to Miss Ghader Miro, Syria for supplying the natural zeolite used in this study.

REFERENCES

- Kragovic M, Dakovic A, Markovic M, Krstic J & Gatta GD (2013). Characterization of lead sorption by the natural and Fe (III)- modified zeolite, *Applied Surface Science*. 283, 764-774.
- Jamil TS, Ibrahim HS, Abd El-Maksoud IH & El-Wakeel, ST (2010). Application of zeolite prepared from Egyptian kaolin for removal of heavy metals: I. Optimum conditions, *Desalination*. 258, 34-40.
- Ennigrou DJ, Ali MB & Dhahbi M (2014). Copper and Zinc removal from aqueous solutions by polyacrylic acid assisted-ultrafiltration, *Desalination*. 343, 82-87.
- Kurniawan T A, Chan GYS, Lo WH & Babel S (2006). Physico-chemical treatment techniques for wastewater laden with heavy metals, *Chemical Engineering Journal*. 118, 83-98.
- Zhu Z, Gao C, Wu Y, Sun L, Huang X, Ran W & Shen Q (2013). Removal of heavy metals from aqueous solution by lipopeptides and lipopeptides modified Nantmorillonite, *Bioresource Technology*. 147, 378-386.
- Breck DW (1974). *Zeolite Molecular Sieves: Structure, Chemistry and Use*. First edition, New York, John Wiley.
- Ibrahim HS, Jamil TS & Hegazy EZ (2010). Application of zeolite prepared from Egyptian kaolin for the removal of heavy metals: II. Isotherm models, *Journal of Hazardous Materials*. 182, 842-847.
- Chaisena A & Rangsrwatananon K (2005). Synthesis of sodium zeolite from natural and modified diatomite, *Materials Letters*. 59, 1474-1479.
- Youssef H, Ibrahim D & Komarneni S (2008). Microwave assisted versus conventional synthesis of zeolite A from metakaolinite, *Microporous and Mesoporous Materials*. 115, 527-534.
- Mousavi SF, Jafari M, Kazemimoghadam M & Mohammadi T (2013). Template free crystallization of zeolite Rho via Hydrothermal synthesis: Effects of synthesis time, synthesis temperature, water content and alkalinity, *Ceramic International*. 39, 7149-7158.
- Katsuki H, Furut S, Watari T & Komarneni S (2005). ZSM-5 zeolite/porous carbon composite: Conventional- and microwave-hydrothermal synthesis from carbonized rice husk, *Microporous and Mesoporous Materials*. 86, 145-151.
- MaY, Alshameri A, Qiu X, Zhou C & li A (2014). Synthesis and characterization of 13X zeolite from low grade natural Kaolinite, *Advanced Powder Technology*. 25, 495-499.
- Belviso C, Cavalcante F, Lettino A & Fiore S (2013). A and X type zeolites from kaolinite at low temperature, *Applied Clay Science*. 80, 162-168.
- Cheng Y, Lu M, Li J, Su X, Pan S, Jiao C & Feng, M (2012). Synthesis of MCM-22 source under varying-temperature conditions, *Journal of Colloid and Interface Science*. 369, 388-394.
- Atta AY, Jibril BY, Aderemi BO & Adefila SS (2012). Preparation of analcime from local kaolin and rice husk ash, *Applied Clay Science*. 61, 8-13.
- Qiu W & Zheng Y (2009). Removal of copper, nickel, cobalt and zinc from water by a cancrinite-type zeolite synthesized from fly ash, *Chemical Engineering Journal*. 145, 483-488.
- Wajima T, Haga M, Kuzawa K, Ishimoto H, Tamada O, Ito K, Nishiyama T, Downs RT & Rakovan JT (2006). Zeolite synthesis from paper sludge ash at low temperature (90°C) with addition of diatomite, *Journal of Hazardous Materials*. 132, 244-252.
- Petkowicz DI, Rigo RT, Radtke C, Pergher, SB & Dos-Santos J. H (2008). Zeolite NaA from Brazilian chrysotile and rice husk, *Microporous and Mesoporous Materials*. 116, 548-554.
- Liu H, Shen T, Yuan P, Shig & Bao X (2014). Green synthesis of zeolites from a natural aluminosilicate mineral rectorite: Effects of thermal treatment temperature, *Applied Clay Science*. 90, 53-60.
- Xing-dong L, Yi-pin W, Xue-min C, Yan H & Jin M (2013). Influence of synthesis parameters on NaA zeolite crystal, *Powder Technology*. 243, 184-193.
- Gougazeh M & Buhl JC (2014). Synthesis and characterization of zeolite A by hydrothermal transformation of natural Jourdanian Kaolin, *Journal of the Association of Arab Universities for Basic and Applied Sciences*. 15, 35-42.

22. Pitcher SK, Slade R.C & Ward N.I (2004). Heavy metal removal from motorway stormwater using zeolites, *Science of the Total Environment*. 334-335,161-166.
23. Treacy M & Higgins JB (2001). *Collection of Simulated XRD Powder Patterns for Zeolites*, Elsevier, Amsterdam.
24. Mohamed RM, Ismail AA, Kini G, Ibrahim IA, Koopman B (2009). Synthesis of highly ordered cubic zeolite A and its ion exchange behavior, *Colloids and Surfaces A: Physicochemical and Engineering Aspects*. 348,87-92.
25. Seliem MK, Komarneni S, Byrne T, Cannon FS, Shahien MG, Khalil AA & Abd El-Gaid IM (2013). Removal of Perchlorate by synthetic organosilica and organoclays: Kinetic and Isotherm Studies, *Applied Clay Science*. 71, 21-26.
26. El-Mekkawi DM & Selim M (2014). Removal of Pb²⁺ from water by using Na-Y zeolites prepared from Egyptian kaolins collected from different sources, *Journal of Environmental Chemical Engineering*. 2, 723-730.
27. Mehdizadeh S, Sadjadi S, Ahmadi SJ & Outokesh M (2014). Removal of heavy metals from aqueous solution using platinum nanoparticles/Zeolite-4A, *Journal of Environmental Health Science & Engineering*. 12, 1-7.
28. Mishra PC & Patel RK (2009). Removal of lead and zinc ions from water by low cost adsorbents, *Journal of Hazardous Materials*. 168, 319–325.
29. Vaca-Mier M, Callejas RL, Gehr R, Cisneros BEJ & Alvarez PJ J (2001). Heavy metal removal with Mexican clinoptilolite: multi-component ionic exchange, *Water Research*. 35, 373–378.
30. Zeng Y, Woo H, Leeg & Park J (2010). Removal of chromate from waste water using surfactant modified Pohang clinoptilolite and Haruna chabazite, *Desalination*. 257, 102-109.
31. Demiral H & Gunduzoglu (2010). Removal of nitrate from aqueous solutions by activated carbon prepared from sugar beet bagasse, *Bioresource Technology*. 101,1675-1680.
32. Reo MM, Reog P, Sesaiah K, Choudary NV & Wang MC (2008). Activated carbon from *Ceiba Pentandra* hulls, an agricultural waste, as an adsorbent in the removal of lead and zinc from aqueous solutions, *Waste management*. 28, 849-858.
33. Zhang H, Tong Z, Wei T & Tang Y (2011). Removal characteristics of Zn (II) from aqueous Solution alkaline Ca-bentonite, *Desalination*. 276, 103-108.
34. Oren AH & Kaya A (2006). Factors affecting adsorption characteristics of Zn²⁺ on two natural zeolites, *Journal of Hazardous Materials*. B131, 59-65.
35. Wang Y, Gao BY, Yue WW & Yue QY (2007). Adsorption kinetics of nitrate from aqueous solutions onto modified wheat residue, *Colloids and Surfaces A: Physicochem. Eng. Aspects*. 308, 1-5.
36. Hoda N, Bayram E & Ayranci E (2006). Kinetic and equilibrium studies on the removal of acid dyes from aqueous solutions by adsorption onto activated carbon cloth, *Journal of Hazardous Materials*. B 137, 344-351.
37. Bagherifam S, Komarneni S, Lakzianb A, Fotovat A, Khorasani R, Huang W, Ma J, Hong S, Cannon, FS & Wang Y (2014). Highly selective removal of nitrate and perchlorate by organoclay, *Applied Clay Science*. 95, 126-132.
38. Lian L, Guo L & Guo C (2009). Adsorption of Congo red from aqueous solutions onto Ca-bentonite, *Journal of Hazardous Materials*. 161, 126-131.
39. Wang S & Zhu ZH (2006). Characterization and environmental application of an Australian natural zeolite for basic dye removal from aqueous dye solution, *Journal of Hazardous Materials*. 136, 946-952.
40. Amin NK (2008). Removal of reactive dye from aqueous solutions by adsorption onto activated carbons prepared from sugarcane bagasse pith, *Desalination*. 223, 152–161.
41. Vimonses V, Lei S, Jin B, Chow CW K & Saint C (2009). Adsorption of Congo red by three Australian kaolins, *Applied Clay Science*. 43, 465- 472.

CITE THIS ARTICLE AS:

Moaz K. Seliem, E.A. Mohamed, A.Q. Selim, M. G. Shahien, Mostafa R. Abukhadra. Synthesis of NA-A Zeolites from Natural and Thermally Activated Egyptian Kaolinite: Characterization and Competitive Adsorption of Copper Ions from Aqueous Solutions. *International Journal of Bioassays* 4.10 (2015): 4423-4430.

Source of support: Beni-Suef University, Egypt

Conflict of interest: None Declared